# DEEP LEARNING BASED ACTIVE CONTOUR ALGORITHMS FOR DIABETIC RETINOPATHY SEGMENTATION

by

RAGHAVKUMAR THAKKAR

A project report submitted in conformity with the requirements
for the degree of Master of Science, Information Technology

Department of Mathematical and Physical Sciences
Faculty of Graduate Studies
Concordia University of Edmonton

**DEEP LEARNING BASED ACTIVE CONTOUR ALGORITHMS FOR DIABETIC RETINOPATHY SEGMENTATION**

**RAGHAVKUMAR THAKKAR**

**Approved:**

---

Supervisor: Baidya Nath Saha, Ph. D. Date

---

Committee Member Date

---

Dean of Graduate Studies: Alison Yacyshyn, Ph. D. Date

# DEEP LEARNING BASED ACTIVE CONTOUR ALGORITHMS FOR DIABETIC RETINOPATHY SEGMENTATION

RAGHAVKUMAR THAKKAR
Master of Science, Information Technology
Department of Mathematical and Physical Sciences
Concordia University of Edmonton
2022

## Abstract

Active contour is one of successful image segmentation techniques, which has been implemented in a wide range of medical imaging problems. Active contour minimizes an energy functional in an unsupervised manner, which offers the required force to converge the user defined initial contour at the boundary of the target objects. However, active contour based approaches lack a way to work with labelled images in a supervised machine learning framework. Furthermore, they are unsupervised approaches and success of these methods strongly depend on many parameters, which is selected by empirical results and as a result fail in many real world applications. Inspired from breakthrough successes deep for solving a variety of imaging problems, this research investigates the implementation of active contour models into deep learning framework to increase the segmentation accuracy of the active contour models. Proposed deep learning based active contour algorithms have been successfully implemented on detecting diabetic macular edema, which causes blocking of tiny blood vessels located at the back inner wall of the eye or retina because of high blood sugar content in the blood. In future, we would like to deploy the proposed algorithms in other medical imaging problems and explore the efficacy of different deep architectures for increasing the segmentation accuracy of active contour models.

**Keywords**:Diabetic retinopathy, Diabetic macular edema, Active contour, Medical imaging, Data Preprocessing, machine learning classifiers, Supervised learning, Unsupervised learning

# Contents

# List of Tables

# List of Figures

# Chapter 1

# Introduction

## 1.1 Background

Diabetes affects more than 348 million people worldwide, which includes approximately 1.5 million Canadians, according to the WHO, and it will be the seventh leading cause of death by 2030. Diabetic Retinopathy is an emerging obstacle that causes abnormalities in the retina in diabetic patients. People over the age of 30 who have had diabetes for more than 15 years have a 78 percent chance of developing Diabetic Retinopathy. Diabetic Retinopathy is caused by long-term diabetes mellitus [1]. Retinopathy is defined as retinal damage that causes blood vessels to become choked, leaky, and grow arbitrarily. Diabetic Retinopathy is asymptomatic; it has no effect on vision until it progresses. As a result, screening for Diabetic Retinopathy is critical for both type 1 (non-proliferative) and type 2 (proliferative) diabetic patients, as both are at risk of diabetic Retinopathy. As illustrated in the figure 1.1, there are numerous abnormalities in the retina of diabetic Retinopathy when compared to normal retina.

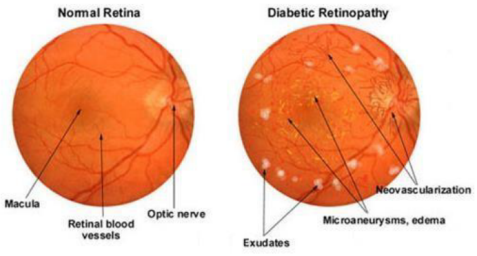


Figure 1.1: Difference between Normal Retina and Diabetic Retinopathy [2]

The most frequent consequence of diabetes mellitus and the main factor in visual loss is diabetic Retinopathy. It is brought on by diabetes-related elevated blood sugar. The portion of your retina that detects light and transmits messages to your brain via a nerve in the back of your eye might become damaged over time if there is

too much sugar in your blood (optic nerve). The retina's blood vessels are harmed throughout by diabetes. When sugar obstructs the minuscule blood arteries leading to your retina, it damages your eyes by causing them to hemorrhage or leak fluid. Due to these obstructed blood arteries, To compensate for these obstructed blood arteries, As shown in the figure 1.2, the eyes then develop new blood vessels that do not function properly. These new blood vessels have a high risk of leaking or bleeding.

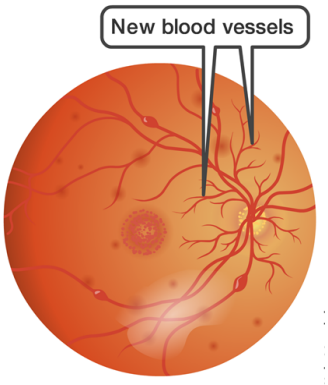


Figure 1.2: Growth of new blood vessel [3]

It has an effect on the blood vessels in the retina (the light-sensitive layer of tissue in the back of your eye). Diabetic Retinopathy may appear without symptoms at first, but detecting it early can help to protect vision. Its etiology and pathology have been extensively studied for more than a half-century, but there are currently few therapeutic options. In the early stages of Retinopathy, symptoms are frequently absent. Some patients experience vision changes, such as difficulty reading or seeing objects in the distance. These adjustments could come and go. Blood vessels in the retina start to bleed into the vitreous in the later stages of the disease (a gel-like fluid that fills in the eye). If this occurs, you might notice cobweb-like black, floaty areas or streaks. The spots may occasionally go away on their own, but it's still crucial to seek medical attention right soon. If the bleeding continues, it may resume, worsen, or leave scarring [4].

Today, an estimated 1.5 Million Canadians identify themselves as having sight loss. An estimated 5.59 million more have an eye disease that could cause sight loss. The Canadian Survey on Disabilities in 2017 provides key statistics about blindness and its impact from coast to coast. The below figure 1.6 includes people who have mild to severe vision loss [5].

The global retinopathy market was valued at USD 6.6 billion in 2021, with a compound annual growth rate of 6.4% expected from 2022 to 2030. Furthermore, according to the Royal National Institute of Blind People (RNIB), diabetic Retinopathy

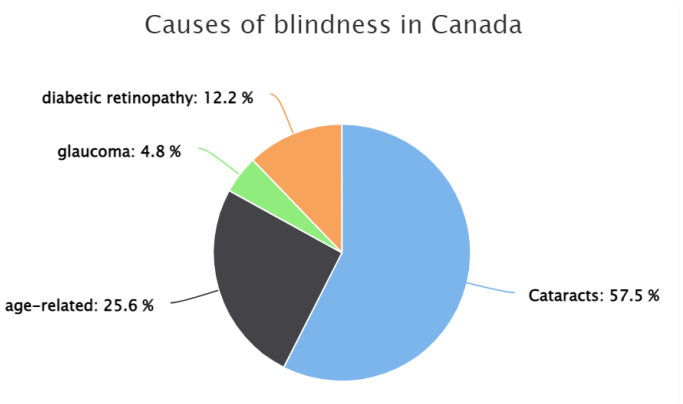


Figure 1.3: Blindness in Canada [5]

was one of the common causes of blindness in the United Kingdom in 2018 [6].

## 1.2 Stages of Diabetic Retinopathy

Diabetic eye disease is classified into two stages.

- Non-Proliferative Diabetic Retinopathy (NPDR)
- Proliferative Diabetic Retinopathy (PDR)

### 1.2.1 Non-Proliferative Diabetic Retinopathy

Non-Proliferative Retinopathy 1.4 is the first stage of diabetic eye disease (NPDR). It is common among diabetics. Tiny blood vessels leak in NPDR, causing the retina to swell. Macular edema occurs when the macula swells. This is the most common cause of diabetes-related vision loss. In addition, NPDR can cause blood vessels in the retina to close. This is known as macular ischemia. Blood cannot reach the macula when this occurs. In the retina, tiny particles known as exudates can form. These can also have an impact on your vision. Anyone who has NPDR will have blurry vision.

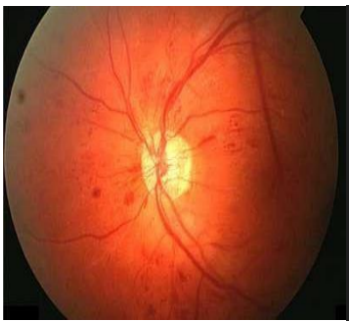

Figure 1.4: An eye was affected by Non-Proliferative Diabetic Retinopathy [1]

### 1.2.2 Proliferative Diabetic Retinopathy

The more advanced stage of retinopathy eye disease is PDR 1.5. It happens when the retina starts to grow new blood vessels. This is referred to as neovascularization. These delicate new vessels bleed into the vitreous on a regular basis. If they only bleed slightly, you may notice a few dark floaters. If they bleed a lot, their vision may be obstructed.

The tissue created by these new blood vessels may scar. Scar tissue has the potential to damage the macula or result in a detached retina. PDR can impair both your central and peripheral (side) vision, which is a very serious issue.

Figure 1.5: A Proliferative Diabetic Retinopathy affected eye [1]

## 1.3 Types of retinal diseases

There are four types of diseases microaneurysms (MA), hemorrhages (HE), hard exudates (EX), and soft exudates (SE). Microaneurysms (MA) were described as circular, small, red dots, while hemorrhages had dots like blot or flame. Soft exudates were defined as light white lesions with somewhat fluffy borders, while hard exudates were yellowish deposits of various shapes and sizes with relatively sharp margins.

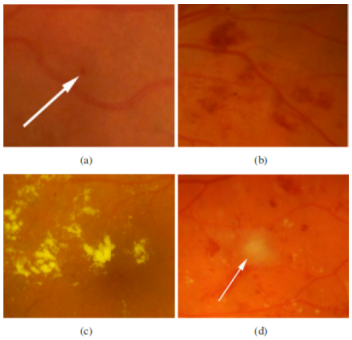


Figure 1.6: Lesions in the eye fundus caused by Diabetic Retinopathy: (a) Microaneurysm (b) Haemorrhages, (c) Hard Exudates, (d) Soft Exudates

## 1.4 Problem Statement

Automatic screening for diabetic Retinopathy can be performed more efficiently and in less time using modern deep learning methods. Because it does not require trained personnel, computer-aided screening reduces costs. Diabetes is one of the world's fastest-growing health threats, and as the number of diabetic patients increases, so does the demand for available infrastructure and resources, necessitating the development of an automatic screening system [7].

Typical manual diagnosis takes 7 to 14 days, as shown in figure 1.7, and needs specialized professionals' input.

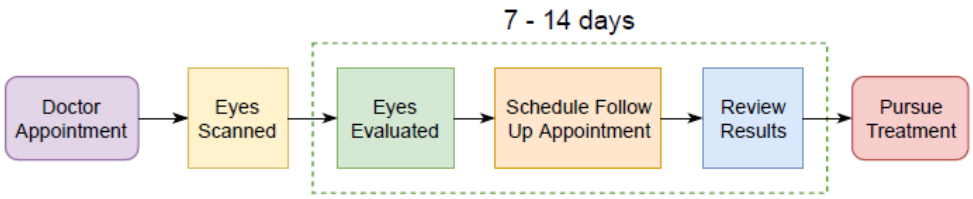


Figure 1.7: Manual diagnosis process

Additionally, Image segmentation has been a hot topic for the image research community over the years, and as a result, it has continued to improve for better implementations in real life.

The purpose of this study is to predict DR and do automated detection of eye diseases microaneurysms (MA), hemorrhages (HE), hard exudates (EX), and soft exudates (SE) based on high-resolution retina images. This will save time in manual diagnosis as well as provide support where specialists are not available. The specific goals of the thesis are as follows:

- Extract disease features from the preprocessed images.
- Detect the presence of Diabetic Retinopathy.
- Classify whether the Diabetic Retinopathy is Proliferative or Non-proliferative.
- Detect the diseases microaneurysms (MA), hemorrhages (HE), hard exudates (EX), and soft exudates (SE).
- Compare the qualitative and quantitative performance of various deep learning models.

## 1.5 Contribution of the thesis

- The research work involves the collection, cleaning, and analysis of data for the extraction of useful insights/information. The contribution to this project work involved the collection of IDRiD. The data collected is about 10 gigabytes which runs into millions of rows. The features of the data were labeled by the expert doctor for each disease.
- The collected data is preprocessed, which involves the removal of special characters, missing values, and stopwords, reducing the data to about 10 million rows of clean data.
- With the machine learning algorithm, feature selection was performed on the data to utilize only features (columns) that give a more accurate analysis of the data. Not all features of the data are relevant for data analysis. Adding irrelevant features to the analysis may result in a less accurate analysis.

## 1.6 Organization of the thesis

There are six (6) chapters in this research work. The first chapter, the Introduction, provides a detailed background of the research work, explaining the reasons for the research work, the problem statement, existing Diabetic Retinopathy detection methods, and the thesis objectives. The second chapter will survey and analyze current methods for detecting diabetic Retinopathy. The methodology for detecting diabetic Retinopathy from retinal fundus images will be discussed in Chapter 3. The dataset used for the experiment will be discussed in Chapter 4. The findings of the analysis will be discussed in Chapter 5. Each step of the analysis is detailed here to help you understand the various insights derived from the data. This research work is concluded in Chapter 6, which also discusses future works for further analysis.

# Chapter 2

# Literature Review

Diabetes patients should be screened on a regular basis because early detection of exudates can help prevent blindness. Manual examination by ophthalmologists, on the other hand, takes time, and the number of experts is insufficient to meet the demand for screening. Given the limitations of manual screening, the prospect of automatic detection of retinal exudates for diagnosis and tracking of a patient's treatment program is appealing. This issue has been addressed several times. Many are based on Machine learning and Deep learning:

## 2.1 Machine learning based approaches

Coria Agurto et al. have proposed the use of multiscale amplitude-modulation-frequency-modulation (AM-FM) methods for discriminating between normal and pathological retinal images. This algorithm allows the user to obtain a detailed analysis of the images since the features are extracted by regions. Then a combination of unsupervised and supervised methods are used for global classification. In this way, all lesions could be detected without the need for manual segmentation by a technician. This method achieves up to 92% accuracy while providing good sensitivity and specificity [8].

Jorge de la Callea et al. explain a technique for finding diabetic retinopathy. This method is broken down into two stages: the first stage uses local binary patterns (LBP) to extract local features, while the second stage employs support vector machines, random forest, and artificial neural networks to do detection. Using a data set of 71 photos, preliminary results demonstrate that random forest was the most accurate classifier with 97.46

Ege B.M. et al. introduced a tool to provide automatic analysis of digital images of diabetic retinopathy. They tested several statistical classifiers, such as Bayesian,

Mahalanobis, and k-nearest neighbors (KNN). Their best results were obtained with the Mahalanobis classifier [9].

Osareh A. et al. introduce an automatic method for the detection of exudate regions. It segmented the color retinal image into homogenous regions using fuzzy C-Means clustering and categorizing the regions into exudates and non-exudates patches using a neural network. According to experimental findings, they reach 92% sensitivity and 82% specificity. [10].

Niemeijer M. et al. provided a method for automatically spotting cotton-wool spots and exudates in digital color fundus images to aid in the early detection of diabetic retinopathy. They employed k-nearest neighbors in their research and reported a receiver operator characteristic curve (ROC) of 0.95 and sensitivity/specificity pairs of 0.95/0.88 for the detection of bright lesions of any type. The corresponding ratios for the detection of exudates, cotton-wool spots, and drusen were 0.95/0.86, 0.70/0.93, and 0.77/0.88 [11].

Silberman N. et al. proposed an automated method for analyzing retinal images to identify diabetic retinopathy. This method recognized exudates with 98.4% accuracy using support vector machines [12].

Neera and Tripathi et al. developed a method for diabetic retinopathy detection based on a local binary pattern and machine learning. This method primarily consists of two steps: the texture operator is used in step one to extract characteristics of diabetic retinopathy. The second level involves the introduction of support vector machines, random forests, and artificial neural networks for detection. The accuracy of random forest is displayed at the first level of results at 94.46% [13].

Mahendran Gandhi et al. have proposed a diagnosis of diabetic retinopathy using morphological operations like erosion followed by dilation for the detection of exudates. Then GLCM features are calculated. Before that, they used preprocessing operations like color space conversion, image restoration, and enhancement operation. Following feature extraction, the image is segmented and applied to the Support Vector Machine (SVM) classifier to categorize it based on the degree of severity. To determine the most accurate method for categorizing photos into distinct categories, such as mild, moderate, or severe retinal scans, this SVM classifier evaluates training data. Images in.jpg format taken by retinal fundus cameras were used to make this diagnosis. And the outcome matched what the ophthalmologist had painstakingly sketched [14].

Sohini Roychowdhury et al. proposed a computer-aided screening system (DREAM) that uses machine learning to score the severity of diabetic retinopathy (DR) using fundus images with different lighting and fields of view. The classification of retinal lesions from non-lesions is examined using classifiers like the Gaussian Mixture Model

(GMM), k-nearest neighbor (kNN), support vector machine (SVM), and AdaBoost. The best classifiers for classifying brilliant and red lesions, respectively, are found to be GMM, and kNN [15].

Li Tang et al. introduced a novel splat feature classification method that was used for hemorrhage detection in retinal fundus images. The whole retinal color images are covered and partitioned into non-overlapping segments. Each partition is called a splat which contains pixels with spatial location and the same color. Each splat consists of retinal features, which are extracted and compared with a variety of filter bank interactions with neighboring splats and texture information and shape. A filtering technique is used to choose the splat features. And then apply the wrapper approach. Given splats along with their associated feature vectors and reference standard labels, these are passed to the classifier for training purposes to detect required objects. Messidor publicly available dataset used in this project. Through this, 0.96 was achieved for the area under the receiver operating characteristic curve at the splat level, and also 0.87 was achieved at the image level [16].

Dr. R. Geetha Ramani et al. proposed a comparative study between two algorithms and compared the result of both algorithms. This comparison happened between two data mining algorithms, i.e., C4.5 (Decision Tree) algorithm versus random tree algorithms. In this comparison, the decision tree gives a better result than the random tree algorithm. C4.5 (Decision Tree) algorithm gives 72% accuracy, and the random tree gives 65% accuracy [17].

L. Giancardo et al. introduced a novel technique that uses uncalibrated multiple-view fundus images to analyze the swelling of the macula. This algorithm was the reconstruction algorithm which contained three steps that were preprocessing containing common operations like greyscale conversion, noise filter, edge detection, and histogram acquisition. The second step that was used was that restoration, and the last step contains the naive height map reconstruction step. This paper worked on the reconstruction concept using the registration method [18].

A new methodology for diagnosing diabetic macular edema (DME) was introduced by Luca Giancardo et al. with the use of a new set of characteristics based on color wavelet decomposition and automatic lesion segmentation. For OEM diagnosis purposes, a single feature vector is developed for each image, and this feature vector is based on three different forms of analysis: the exudates probability map, color analysis, and wavelet analysis. These characteristics are essential for training a classifier that can detect DME by exudation and make an automated diagnosis. The accuracy achieved with the suggested method ranges from 88 to 94 percent [19].

Marwan D. Saleh, C. Eswaran et al. provide an automated system based on

MAs (Microaneurysms) and HAs (Hard exudates) detection, offering an automated decision-support system for non-proliferative diabetic retinal conditions. In this paper, they extract certain crucial elements for precise segmentation of black spot lesions in the fundus pictures, including the optic disc, fovea, and blood vessels. To find aberrant regions like MAs and HAs, the dark object segmentation method is applied. It is customary to assess the degree of diabetic retinopathy, or DR type, in the extremities based on the quantity and distribution of MAs and HAs. Ninety-eight color photos make up the dataset utilized to assess the effectiveness of the provided work. The proposed system achieves 84.31% and 87.53% values in terms of sensitivity for the detection of MAs and HAs and specificity, the system achieves 93.63% and 95.08% values in terms of specificity, respectively. In the development of automated screening systems, the given system leads to Reliable detection of retinal hemorrhages.[20].

LI Yafen et al. have put out a novel strategy utilizing many image processing methods, including texture analysis, picture enhancement, and morphological image processing. SVMs (Support vector machines) classifier is used for classification. It provides an accuracy of 89%, followed by a sensitivity of 90% and specificity of 95%. The Directdb dataset for the fundus image was used in the proposed paper's investigation into the classifier's accuracy [21].

In this research, the exudates were segmented using clustering-based approaches, and the characteristics were extracted using multi-space and color space features by Keerthi Ram et.al. This paper's speed is faster than any other method since it concentrates on the processing time factor. In this, it offers positive predictive values of 87 percent and archives accuracy up to 89.6% [22].

Alireza Osareh et al. employ color normalization and c-mean clustering as pre-processing techniques. In this case, a fuzzy algorithm is used to segment the color image, and characteristics of the retinal image are extracted using a genetic algorithm. This method has good accuracy and sensitivity of 92.2 percent and 93.6 percent, respectively [23].

## 2.2 Deep learning based approaches

Li, Pang, Xiong, and Liu introduced a neural network related to transfer learning for the classification of diabetic retinopathy (DR). Experiments are performed on 1014 and 1200 fundus images from two publicly available DR1 and MESSIDOR datasets. The proposed CNN model consists of seven convolutional layers, two fully connected and a softmax layer. The number of acquired ground-truth data is sometimes insufficient to train the CNNs without overfitting and convergence issues from scratch. Here Results

demonstrate that CNN systems related to transfer learning can reach maximum accuracy with less number of datasets [24].

Jagadish Nayak et al proposed a comparative classifier using two classifiers that are Bayesian statistical classifier and an artificial neural network for the classification of funds images. It used a neural network for the classification of severity of deceases and it gives better results than the Bayesian statistical classifier. The algorithm achieved a sensitivity of 77.5% and specificity of 88.7% for the detection of hemorrhages and microaneurysms. For exudate detection, the sensitivity and specificity were 88.5 and 99.7%, respectively. [25].

Andonov, Pavloviov, Kajan, et al. contributed to image recognition methods that are suitable for diagnostic purposes in ophthalmology. To classify the images according to whether or not they have some types of anomalies, a convolutional neural network (CNN) with four convolutional layers was proposed [26]. According to the figure 2.1, They made use of the MESSIDOR database, which is open to the public.

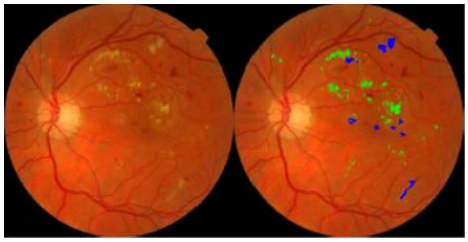

Figure 2.1: Fundus image from database MESSIDOR and image with marked bright lessions (soft - green and hard - blue exudates) by an ophthalmologist. [26]

Matthew Chua et al. provide an automated classification method that uses machine learning models like CNN, VGG-16, and VGG-19 to assess the severity of diabetic retinopathy (DR) based on the analysis of fundus images with different illumination and fields of vision. For classifying pictures into five categories ranging from 0 to 4, where 0 is no DR and 4 is proliferative DR, our system obtains 80

Recently, deep learning-based architectures have become popular and showed good results. Kaggle also launched a competition [27] for DR detection in 2015, where the top-ranked solutions used CNN-based models. In that competition, Kelvin [28] used a pre-trained Inception-V3 model as a baseline and retrained some modified final layers of the CNN with attention to get an accuracy of 60% on the test images. Meena [29] achieved a DR classification accuracy of 74% on the validation dataset using basic preprocessing and a CNN model. Graham [30] achieved the first rank with a score of 84.9%, and he used SparseConvNet CNN and a Random Forest (RF) model to combine predictions from images of the two eyes into a single prediction.

# Chapter 3

# Methodology

This research, diabetic retinopathy is detected using three deep learning models: UNet, ResNet, and DSAC (Deep Structured Active Contours).

## 3.1 UNet (Convolutional neural network)

Medical image processing tools, including computed tomography (CT), X-ray imaging, and magnetic resonance imaging, are now necessary for clinical diagnosis (MRI). Medical image segmentation, a crucial technique for medical image analysis, aids physicians in making accurate decisions and provides a solid foundation for clinical diagnosis and early illness identification.Traditional medical image segmentation algorithms mainly include manual segmentation [31], semi-automatic segmentation [32], and automatic segmentation [33]. These algorithms rely heavily on prior human knowledge and have insufficient generalization ability, making it difficult to achieve satisfactory results.

Deep learning technology's use in medical imaging has recently attracted much interest. One of the challenges that many academics are now interested in is how to automatically distinguish and separate the lesions in medical photos. This issue was addressed by Ronneberger et al. [34] U-Net at the MICCAI conference in 2015, which represented a profound learning innovation in the segmentation of medical imaging. A Fully Convolutional Network (FCN) called U-Net is used to segment biological images. It comprises three modules: an encoder, a bottleneck module, and a decoder. The widely utilized U-Net, with its U-shaped structure combined with context information, quick training speed, and little data usage, satisfies the needs of medical image segmentation. The structure of U-Net is shown in Figure 3.4.

The network architecture is illustrated in Figure 3.4. It comprises an expanded path on the left and a contracting path on the right (right side). The contracting path

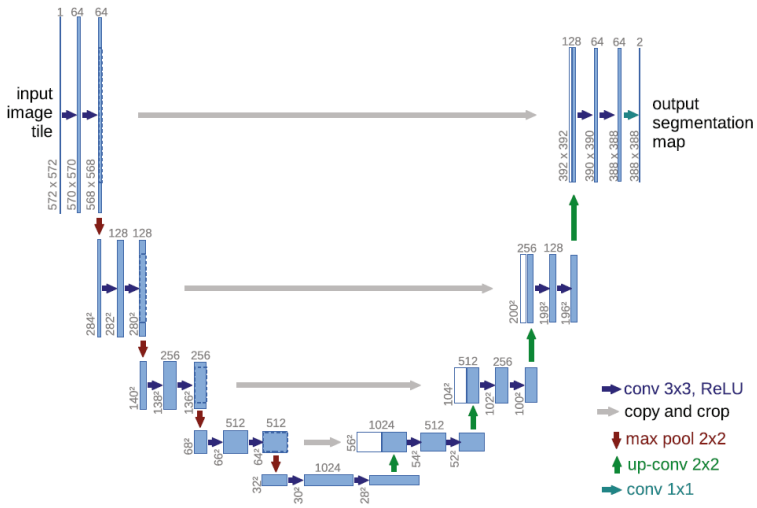


Figure 3.1: U-net architecture (example for 32x32 pixels in the lowest resolution). A multi-channel feature map is represented by each blue box. On top of the box is a sign that indicates the number of channels. At the box's lower left corner, the x-y dimension is provided. Duplicated feature maps are represented by white boxes. Each operation is indicated with an arrow.[34]

adheres to the standard convolutional network architecture. Two 3x3 convolutions (unpadded convolutions) are applied repeatedly, and after each one, a rectified linear unit and a two x two max pooling operation with stride two are applied for downsampling. We quadruple the number of feature channels with each downsampling step. An upsampling of the feature map is followed by a 2x2 convolution ("up-convolution") that cuts the number of feature channels in half, a concatenation with the correspondingly cropped feature map from the contracting path, and two 3x3 convolutions, each followed by a ReLU, at each stage of the expansive path. For the loss of border pixels in each convolution, cropping is required. Each of the 64-component feature vectors is mapped to the desired number of classes in the final layer using a 1x1 convolution. The network includes 23 convolutional layers altogether [35].

UNET augments the available training images with excessive data by applying elastic deformations. This enables the network to learn invariance to such deformations without having to see them in the annotated image corpus [36]. This is important in biomedical segmentation because deformation was previously the most common variation in tissue, and realistic deformations can be efficiently simulated.

UNET has a high level of accuracy for CT scans and X-ray disease detection, as well as for cell-level disease detection [37]. I choose UNET to detect diabetic retinopathy because of its high accuracy with less training dataset and pixel-level disease localization.

## 3.2 Residual Networks (ResNet)

Following the first CNN-based architecture (AlexNet), which won the ImageNet 2012 competition, each subsequent winning architecture employs more layers in a deep neural network to reduce error rates. This works for fewer layers, but as the number of layers increases, we encounter a common problem in deep learning known as the Vanishing or Exploding gradient. This results in the gradient becoming 0 or being overly large [38]. The training and testing error rate rises with the number of layers.

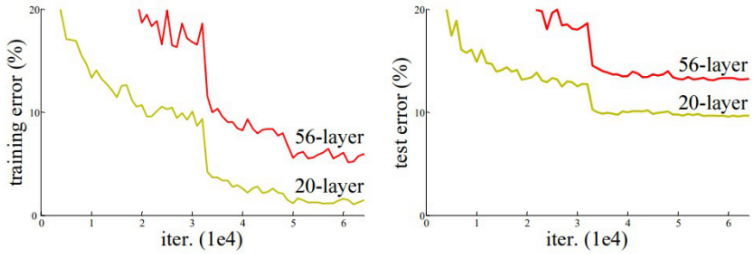


Figure 3.2: Comparison of 20-layer vs. 56-layer architecture. [39]

In the above plot 3.2, we can see that a 20-layer CNN design outperforms a 56-layer CNN in terms of error rate on both training and testing datasets. The authors came to the conclusion that the error rate is driven by vanishing/exploding gradient after conducting further analysis.[40]. 2015 saw the introduction of ResNet by Microsoft Research professionals, who also labeled it a unique architecture.

This design developed the Residual Blocks concept to deal with the vanishing/exploding gradient issue. This network uses a technique called skip connections. The skip connection ignores some levels in between to link layer activations to subsequent layers [39]. Consequently, a block is left over. To build resents, these leftover blocks are piled. Instead of having layers learn the underlying mapping, the approach used by this network is to let the network fit the residual mapping. So, rather than using, for example, the initial mapping of H, let the network fit (x).

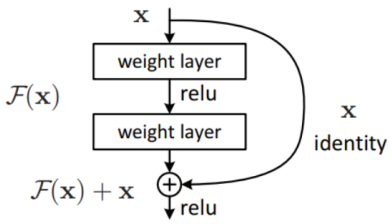


Figure 3.3: Skip (Shortcut) connection [41]

The advantage of including this type of skip connection is that if any layer degrades

architecture performance, it will be skipped by regularisation. As a result, training a very deep neural network is possible without the issues caused by vanishing/exploding gradients. The researchers conducted experiments on 100-1000 layers of the CIFAR-10 dataset. A similar approach is known as "highway networks," and these networks, too, use skip connections. These skip connections, like LSTM, make use of parametric gates. These gates control how much data passes through the skip connection.

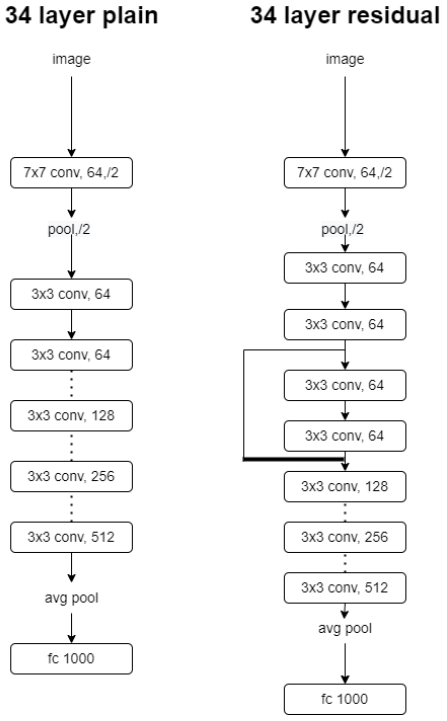


Figure 3.4: Skip (Shortcut) connection

This network uses a 34-layer plain network architecture inspired by VGG-19, in which then the shortcut connection is added. These shortcut connections then convert the architecture into a residual network.

## 3.3 Deep Structured Active Contours(DSAC)

Medical image segmentation is critical for clinical diagnosis and image analysis. Convolutional neural networks (CNNs) have recently achieved tremendous success in this task; however, they perform poorly at recognizing precise object boundaries due to information loss in successive downsampling layers. To address this issue, we combine an active contour model (convexified Chan-Vese model) with the CNN structure (DenseUNet), resulting in a new framework known as a deep active contour network (DACN). Instead of manual configuration, DACN employs a CNN backbone to

automatically learn the initialization and parameters of an active contour model (ACM). The proposed DACN takes advantage of ACM to accurately detect object boundaries, which can be trained in an end-to-end differential manner. The experimental results on two public datasets demonstrate the effectiveness of DACN, and the trimap experiment confirms the superior ability of DACN to obtain precise boundary delineation [42].

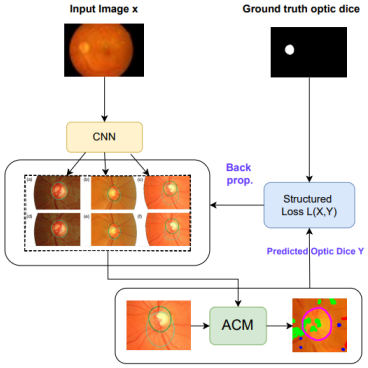


Figure 3.5: Deep Structured Active Contours

As shown in the above figure 3.5, Image x is fed into the CNN model, which attempts to draw a contour around the optic dice. The output will then be sent to the active contour model, which will draw a smooth contour to the optic dice. I also tweaked the loss function to better match the accuracy to the ground truth.

Because the active contour is a type of segmentation technique that uses energy forces and constraints to separate the pixels of interest from an image for further processing and analysis, act Active contour is defined as an active model for the segmentation process. Thus, an active contour gives good accuracy in detecting diabetic retinopathy in the early stage.

# Chapter 4

# Data Collection and Preprocessing

## 4.1 Data Collection

The IDRiD (Indian Diabetic Retinopathy Image Dataset) dataset for diabetic retinopathy is the first to be representative of an Indian population. Furthermore, it is the only dataset that includes both typical diabetic retinopathy lesions and normal retinal structures annotated at the pixel level. For each image, this dataset contains information on the disease severity of diabetic retinopathy and diabetic macular edema. As a result, it is ideal for the development and testing of image analysis algorithms for the early detection of diabetic retinopathy.

This dataset was made accessible in conjunction with the IEEE International Symposium on Biomedical Imaging (ISBI-2018), Washington D.C., as part of the "Diabetic Retinopathy: Segmentation and Grading Challenge [43].

The IDRiD dataset is a brand-new, freely accessible database of 516 retinal fundus photographs that are divided into two categories.

- Retinal images with the signs of D.R. and/or DME.
- Normal retinal images (without signs of D.R. and/or DME).

The dataset offers ground truths related to normal retinal architecture, as well as the symptoms of diabetic retinopathy (D.R.) and diabetic macular edema (DME), which are listed below and defined as follows:

- Pixel level annotations of typical diabetic retinopathy lesions and optic disc.
- Image level disease severity grading of diabetic retinopathy and diabetic macular edema.
- Optic Disc and Fovea center coordinates.

### 4.1.1 Pixel Level Annotated Data

This collection includes 164 color fundus images without D.R. and 81 color fundus images with DR. For the purpose of evaluating the effectiveness of individual lesion segmentation algorithms, precise pixel-level annotation of abnormalities associated with D.R., such as microaneurysms (M.A.), soft exudates (S.E.), hard exudates (EX), and hemorrhages (HE), is provided as a binary mask. It includes different binary masks for each type of lesion and color fundus photos (.jpg files) (.tif files). For all 81 photos, it also includes an optic disc (O.D.) mask in addition to the lesion masks (see an example in Figure ).

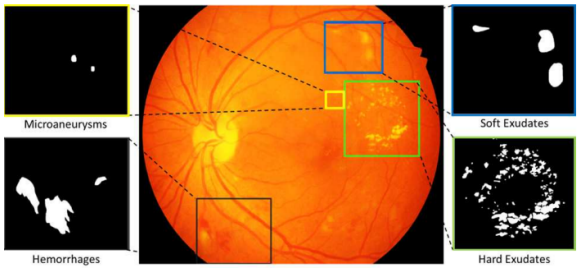


Figure 4.1: Color fundus photograph containing different retinal lesions associated with diabetic retinopathy. Enlarged parts illustrating sample annotations of Microaneurysms, Soft Exudates, Hemorrhages, and Hard Exudates [44]

### 4.1.2 Image Level Disease Grading

The medical experts graded the full set of 516 images with a variety of pathological conditions of D.R. and DME. The dataset is divided into two parts training and testing set comprising 413 (80%) and 103 (20%) images, respectively, by maintaining an appropriate mixture of disease stratification. Similarly, the expert labels of D.R. and DME severity levels for the dataset are provided in two CSV files.

- IDRiD_DiseaseGrading_TrainingLabels.CSV
- IDRiD_DiseaseGrading_TestingLabels.CSV

Figure 4.2 illustrates the information available in both CSV files with each column description given as follows:

1. Image No: Name (serial number) of identified and renamed patient image.
2. DR Grade: D.R. severity level in range 0 (No apparent D.R.) to 4 (Severe DR).
3. Risk of DME: Macular edema severity level in range 0 (No DME) to 2 (Severe DME).

| | A | B | C |
|---|---|---|---|
| 1 | Image No | DR Grade | Risk of DME |
| 2 | IDRiD_001 | 3 | 1 |
| 3 | IDRiD_002 | 2 | 2 |
| 4 | IDRiD_003 | 4 | 2 |
| 5 | IDRiD_004 | 2 | 1 |
| 6 | IDRiD_005 | 1 | 0 |

Figure 4.2: Sample D.R. and DME expert labels in CSV file

| Data | Description | Quality |
|---|---|---|
| Color Fundus Images of Retina | Raw Data | 516 |
| Disease Severity Grading of D.R. and DME | Image level Grading | 516 |
| Center coordinates of OD and Fovea | Manual center co-ordinates | 516 |
| Binary Mask of different lesions | Precise pixel level manual annotation | 81 |
| Binary Mask of the optic disc | Precise pixel level manual annotation | 81 |

Table 4.1: Date and Description

### 4.1.3 Optic Disc and Fovea Center Location

Along with the annotations presented above, the dataset provides center pixel locations of the optic disc [ODx, ODy] and fovea [Fx, Fy] for all 516 images, as shown in Figure 4.

The dataset is divided into two parts training and testing set comprising 413 (80%) and 103 (20%) images, respectively. Center pixel markups for O.D. and Fovea are made available in two separate folders.

The table summarizes the available data with its description, quantity of data, and different file types.

## 4.2 Preprocessing

The Preprocessing has been done in two steps. The first one is general preprocessing, which is applied to all the images of the dataset. The second one is the specific preprocessing according to the features to be extracted [44].

### 4.2.1 General Preprocessing

- Resizing

  In this work, the sizes of the actual images are 4288X2848 pixels. As the dataset is huge in size, one image is cropped into small images in .jpeg format with a size of 512x512 pixels to reduce the computational time. Which also helps to detect disease in a particular section of the eye [44].

- Green Channel Extraction

  Preprocessing of the fundus image is performed in order to improve the contrast. In order to improve the contrast of the retinal images, some information is commonly discarded before processing, such as the red and blue components of the image. Green channel is extensively used in preprocessing as it displays the best vessels/background contrast and the greatest contrast between the optic disc and retinal tissue. The red channel is relatively bright, and the vascular structure of the choroid is visible. The retinal vessels are also visible but show less contrast than a green channel. The Blue channel is noisy and contains little information [44].

- Contrast Limited Adaptive Histogram Equalization

  CLAHE (Contrast Limited Adaptive histogram equalization) is getting used for contrast enhancement. CLAHE computes several histograms of an image and uses them to reallocate the intensity value of an image. Hence, CLAHE is more appropriate to improve regional contrast and edge enhancement in each region of the image [44].

### 4.2.2 Specific Preprocessing

The specific preprocessing is performed for exudate detection by using morphological processes, median filtering, and thresholding.

- Exudate Detection

  Using a 6x6 ellipse-shaped structuring element, morphological dilation is applied. The nonlinear median filter is used for noise removal. Exudates are in high-intensity values. So it has been extracted using thresholding. After applying this preprocessing, pixels having intensity values higher than 235 are set to 255, and the rest of them are set to 0. Then traversing the image, the area of exudates is calculated [44].

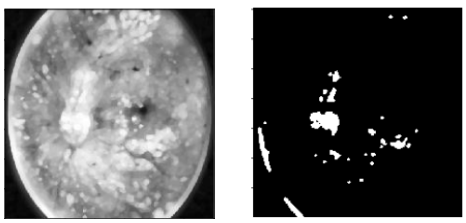

Figure 4.3: Steps of Exudate detection

- Blood Vessel Detection:

The blood vessel is one of the important features for differentiating diabetic retinopathy stages. After obtaining the green channel image and improving the contrast of the image, several steps have been taken to extract blood vessels. Alternate sequential filtering (three times opening and closing) using three different sized and ellipse-shaped structural elements, 5x5, 11x11, and 23x23, is applied to the image. Then the resultant image is removed from the input image. Subtracted image has lots of small noises. Those noises are removed through area parameter noise removal. Contours of each component, including noises, are found by using the function find contours( ) and calculating the contour area by using the function contour area( ) and removing the noises having more than or equal to 200 pixels as area. Then the resultant image is binarized using a threshold value. Finally, the number of pixels that covers the blood vessel area is calculated [44].

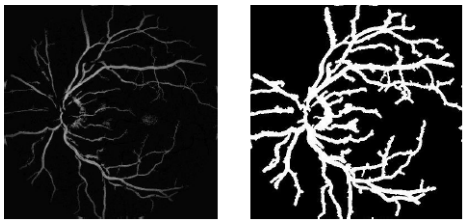

Figure 4.4: Steps of Exudate detection

- Microaneurysm Detection The green component of the RGB value is used to extract microaneurysm. For better contrast, CLAHE is used. Then the median filter is used for noise removal. 7x7 ellipse-shaped structural element is used for morphological operation. Morphological operation erosion is applied, and then the image is inverted. For joining the disjoint segments of the blood vessel, morphological closing is used. Then the image was binarized. As the blood vessel, hemorrhage and microaneurysm have almost the same intensity, all these components will be detected altogether in the binarized image. Since microaneurysm is smaller in size [44].

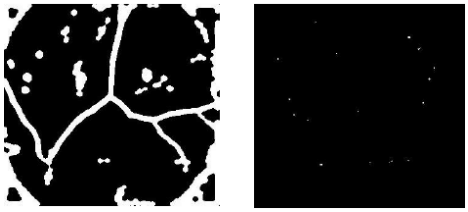

Figure 4.5: Steps of Blood Vessel detection

# Chapter 5

# Results and Discussions

A color fundus image of the eye is provided as an input, and by processing this, we get the result of whether the eye is affected by Diabetic Retinopathy. To detect Diabetic Retinopathy, we preprocess the image and apply classification techniques. We divide the total process into three steps- preprocessing, feature extraction, and Diabetic Retinopathy classification. Preprocessing includes copping images and creating a label of the cropped image. In the feature extraction phase, we extract several features like the area of exudates, area of blood vessels, area of microaneurysm, etc. Finally, in the classification phase, we will detect whether Diabetic Retinopathy is present or not. Moreover, if present, Detect the diseases microaneurysms (MA), hemorrhages (HE), hard exudates (EX), and soft exudates (SE).

### 5.0.1 Experimental Setup

To perform our work, Diabetic Retinopathy Classification from Retinal Images using Machine Learning Approach, we have used a computer with a decent configuration as an experimental setup. For our thesis, we have used the following configuration as an experimental setup.

- Intel Xeon Processor
- 516GB RAM
- 1TB Hard-disc
- NVIDIA Corporation GV100GL [Tesla V100 PCIe 16GB]
- Jupyter Notebook

### 5.0.2 Experimental Result and Analysis

There are two types of performance evaluation: qualitative performance evaluation and quantitative performance evaluation.

In our thesis work, we calculated both quantitative and qualitative work. Our work is graded on accuracy, sensitivity, and specificity. We calculated the Jaccard Score, Dice Coefficient, and Parts figure of merit for each disease and compared the accuracy of each algorithm.

- Jaccard Score

  The Jaccard Score is a popular proximity metric that is used to determine how similar two objects—like two texts—are to one another. You can use the Jaccard similarity to determine whether two asymmetric binary vectors or two sets are similar. Other names for the concept of Jaccard similarity, represented by, are Jaccard Index, Jaccard Coefficient, Jaccard Dissimilarity, and Jaccard Distance [45].

- Dice Coefficient

  A predicted segmentation's pixel-by-pixel agreement with the associated ground truth can be compared using the Dice coefficient. The dice coefficient is two. The area of overlap is divided by the sum of all pixels in both photos [45].

- Partts figure of merit

  Figures of merit are numerical metrics that are frequently used to compare the detection and prediction abilities of analytical techniques. A prominent area of research in recent years is the determination of analytical figures of merit for calibrations based on first- and higher-order data [45].

### 5.0.3 Qualitative Performance Evaluation

As shown in 5.1, For each disease, I compared the UNET, ResNet, and DSAC models. UNET detects hard exudates and hemorrhages with greater accuracy than other models. ResNet detects optical discs with greater precision than other models. Microaneurysms and Soft Exudates are detected more precisely in DSAC.

### 5.0.4 Quantitative Performance Evaluation

- Hard Exudates

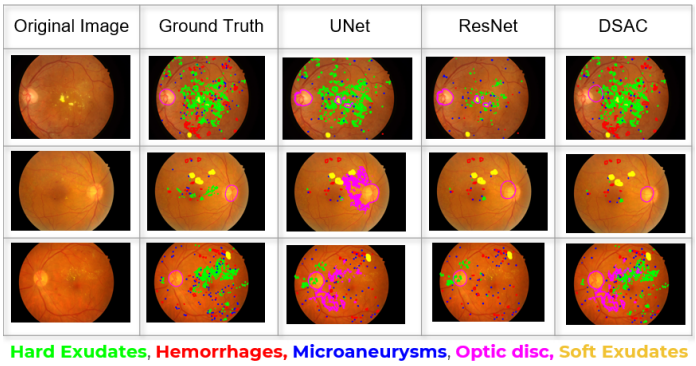


Figure 5.1: Qualitative Performance Evaluation

As shown in below figure, UNET detects hard exudates with greater accuracy than other models.

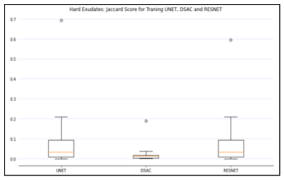

Figure 5.2: Jaccard Score

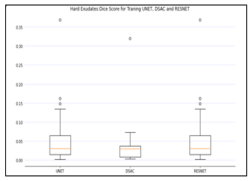

Figure 5.3: Dice Coefficient

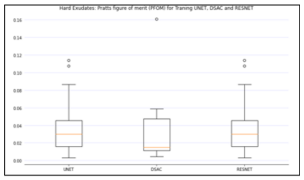

Figure 5.4: Partts figure of merit

- Hemorrhages

  As shown in below figure, UNET detects Hemorrhages with greater accuracy than other models.

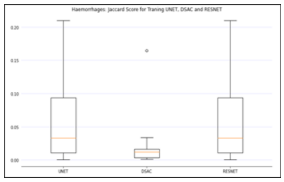

Figure 5.5: Jaccard Score

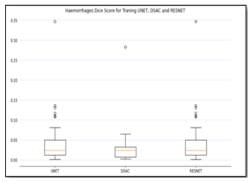

Figure 5.6: Dice Coefficient

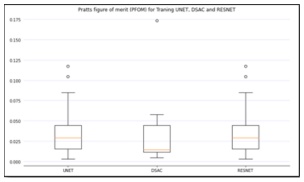

Figure 5.7: Partts figure of merit

- Microaneurysms

  As shown in below figure, DSAC detects Microaneurysms with greater accuracy than other models.

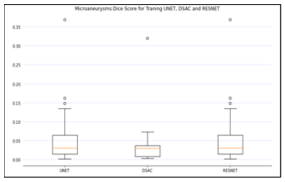

Figure 5.8: Jaccard Score

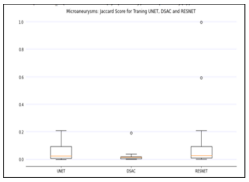

Figure 5.9: Dice Coefficient

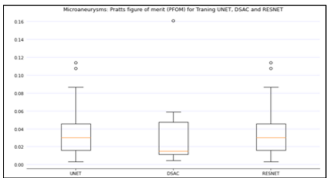

Figure 5.10: Partts figure of merit

- Optic disc

  As shown in below figure, ResNet detects Optic disc with greater accuracy than other models.

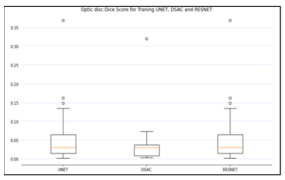

Figure 5.11: Jaccard Score

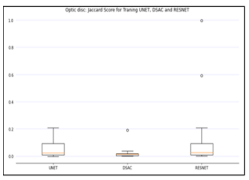

Figure 5.12: Dice Coefficient

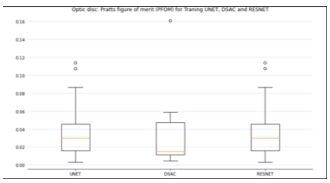

Figure 5.13: Partts figure of merit

# Chapter 6

# Conclusion and Future Works

We get the conclusion that our suggested technique successfully detects diabetic retinopathy after looking at the current systems. I identified diabetic retinopathy using three deep learning models: Unet, ResNet, and Deep Structured Active Contours (DSAC). Using benchmark datasets that are available to the public. Unet outperforms other deep learning models. The Pratts figure of merit, dice coefficient, and Jaccard score was used to assess the effectiveness of various models.

In the near future, I want to create a web application solution that takes an image as input and outputs the type of disease. I will also compare it to other Deep Learning models in order to improve segmentation performance, particularly the loss function of the deep active contour method. Currently, I am implementing an automated machine learning-based disease grading method that defines disease stages. I'm also competing in the MICCIA medical imaging competition [46].

# Bibliography


[1] T. Mahmud and I. Bhattacharjee, "Diabetic retinopathy classification from retinal images using machine learning approaches," 2020.

[2] P. Kapoor and S. Arora, "Applications of deep learning in diabetic retinopathy detection and classification: A critical review," in *Proceedings of Data Analytics and Management*, D. Gupta, Z. Polkowski, A. Khanna, S. Bhattacharyya, and O. Castillo, Eds., Singapore: Springer Singapore, 2022, pp. 505–535, ISBN: 978-981-16-6285-0.

[3] S. staff, *Eye damage and diabetes*, 2022. DOI: 10.48550/ARXIV.1911.05861. [Online]. Available: https://www.aboutkidshealth.ca/article?contentid=2522&language=english#.

[4] *Diabetic-retinopathy*, 2020. [Online]. Available: https://www.nei.nih.gov/learn-about-eye-health/eye-conditions-and-diseases/diabetic-retinopathy.

[5] *Blindness-canada*. [Online]. Available: https://cnib.ca/en/sight-loss-info/blindness/blindness-canada?region=ab.

[6] *Industry-analysis*, 2020. [Online]. Available: https://www.grandviewresearch.com/industry-analysis/diabetic-retinopathy-market.

[7] *Who-analysis*. [Online]. Available: https://www.who.int/news-room/fact-sheets/detail/diabetes.

[8] C. Agurto, V. Murray, E. Barriga, *et al.*, "Multiscale am-fm methods for diabetic retinopathy lesion detection," *IEEE Transactions on Medical Imaging*, vol. 29, no. 2, pp. 502–512, 2010. DOI: 10.1109/TMI.2009.2037146.

[9] B. Ege, O. Hejlesen, O. Larsen, *et al.*, "Screening for diabetic retinopathy using computer based image analysis and statistical classification," *Computer methods and programs in biomedicine*, vol. 62, pp. 165–75, Aug. 2000. DOI: 10.1016/S0169-2607(00)00065-1.

[10] A. Osareh, M. Mirmehdi, and B. Thomas, "Automatic recognition of exudative maculopathy using fuzzy c- means clustering and neural networks," Nov. 2001.

[11] M. Niemeijer, B. Ginneken, S. Russell, M. Suttorp-Schulten, and M. Abràmoff, "Automated detection and differentiation of drusen, exudates, and cotton-wool spots in digital color fundus photographs for diabetic retinopathy diagnosis," *Investigative ophthalmology visual science*, vol. 48, pp. 2260–7, Jun. 2007. DOI: 10.1167/iovs.06-0996.

[12] N. Silberman, K. Ahrlich, R. Fergus, and L. Subramanian, "Case for automated detection of diabetic retinopathy.," Jan. 2010.

[13] S. Neera and R. Tripathi, "Automated early detection of diabetic retinopathy using image analysis techniques," *International Journal of Computer Applications*, vol. 8, Oct. 2010. DOI: 10.5120/1186-1648.

[14] M. Gandhi and R. Dhanasekaran, "Diagnosis of diabetic retinopathy using morphological process and svm classifier," in *2013 International Conference on Communication and Signal Processing*, 2013, pp. 873–877. DOI: 10.1109/iccsp.2013.6577181.

[15] S. Roychowdhury, D. D. Koozekanani, and K. K. Parhi, "Dream: Diabetic retinopathy analysis using machine learning," *IEEE Journal of Biomedical and Health Informatics*, vol. 18, no. 5, pp. 1717–1728, 2014. DOI: 10.1109/JBHI.2013.2294635.

[16] L. Tang, M. Niemeijer, J. M. Reinhardt, M. K. Garvin, and M. D. Abramoff, "Splat feature classification with application to retinal hemorrhage detection in fundus images," *IEEE Transactions on Medical Imaging*, vol. 32, no. 2, pp. 364–375, 2013. DOI: 10.1109/TMI.2012.2227119.

[17] R. G. Ramani, B. Lakshmi, and S. G. Jacob, "Data mining method of evaluating classifier prediction accuracy in retinal data," in *2012 IEEE International Conference on Computational Intelligence and Computing Research*, 2012, pp. 1–4. DOI: 10.1109/ICCIC.2012.6510290.

[18] L. Giancardo, F. Meriaudeau, T. P. Karnowski, *et al.*, "Textureless macula swelling detection with multiple retinal fundus images," *IEEE Transactions on Biomedical Engineering*, vol. 58, no. 3, pp. 795–799, 2011. DOI: 10.1109/TBME.2010.2095852.

[19] L. Giancardo, F. Meriaudeau, T. Karnowski, *et al.*, "Exudate-based diabetic macular edema detection in fundus images using publicly available datasets," *Medical image analysis*, vol. 16, pp. 216–26, Jul. 2011. DOI: 10.1016/j.media.2011.07.004.

[20] M. Saleh and C. Eswaran, "An automated decision-support system for non-proliferative diabetic retinopathy disease based on mas and has detection," *Computer methods and programs in biomedicine*, vol. 108, pp. 186–96, Apr. 2012. DOI: 10.1016/j.cmpb.2012.03.004.

[21] N. Du and Y. Li, "Automated identification of diabetic retinopathy stages using support vector machine," in *Proceedings of the 32nd Chinese Control Conference*, 2013, pp. 3882–3886.

[22] K. Ram and J. Sivaswamy, "Multi-space clustering for segmentation of exudates in retinal color photographs," in *2009 Annual International Conference of the IEEE Engineering in Medicine and Biology Society*, 2009, pp. 1437–1440. DOI: 10.1109/IEMBS.2009.5332911.

[23] A. Osareh and B. Shadgar, "A computational-intelligence-based approach for detection of exudates in diabetic retinopathy images," *IEEE transactions on information technology in biomedicine : a publication of the IEEE Engineering in Medicine and Biology Society*, vol. 13, pp. 535–45, Aug. 2009. DOI: 10.1109/TITB.2008.2007493.

[24] X. Li, T. Pang, B. Xiong, W. Liu, P. Liang, and T. Wang, "Convolutional neural networks based transfer learning for diabetic retinopathy fundus image classification," in *2017 10th International Congress on Image and Signal Processing, BioMedical Engineering and Informatics (CISP-BMEI)*, 2017, pp. 1–11. DOI: 10.1109/CISP-BMEI.2017.8301998.

[25] J. Nayak, P. Bhat, U. R. Acharya, C. Lim, and M. Kagathi, "Automated identification of diabetic retinopathy stages using digital fundus images," *Journal of medical systems*, vol. 32, pp. 107–15, Apr. 2008. DOI: 10.1007/s10916-007-9113-9.

[26] M. Andonová, J. Pavlovičová, S. Kajan, M. Oravec, and V. Kurilová, "Diabetic retinopathy screening based on cnn," in *2017 International Symposium ELMAR*, 2017, pp. 51–54. DOI: 10.23919/ELMAR.2017.8124433.

[27] K. 2. D. R. Detection., *Eye damage and diabetes*, 2015. DOI: https://www.kaggle.com/c/diabetic-retinopathy-detection/overview. [Online]. Available: https://www.kaggle.com/c/%20diabetic-retinopathy-detection/overview.

[28] ——, *Kaggle diabetic retinopathy detection competition report*, 2015. [Online]. Available: https://www.kaggle.com/kmader/inceptionv3-for-retinopathy-gpu-hr.

[29] ——, *Kaggle diabetic retinopathy detection competition report*, 2015. [Online]. Available: https://www.kaggle.com/meenavyas/diabetic-retinopathy-detection.

[30] ——, *Kaggle diabetic retinopathy detection competition report*, 2015. [Online]. Available: https://www.kaggle.com/c/diabetic-retinopathy-detection/discussion/15801.

[31] N. Mudigonda, R. Rangayyan, and J. Desautels, "Gradient and texture analysis for the classification of mammographic masses," *IEEE Transactions on Medical Imaging*, vol. 19, no. 10, pp. 1032–1043, 2000. DOI: 10.1109/42.887618.

[32] H.-D. Cheng, X. Shi, R. Min, L. Hu, X. Cai, and H. Du, "Approaches for automated detection and classification of masses in mammograms," *Pattern recognition*, vol. 39, no. 4, pp. 646–668, 2006.

[33] B. Qi, H. Li, X. Pan, and Y. Kang, "Breast mass segmentation in mammography using improved dynamic programming," in *2012 IEEE International Conference on Information and Automation*, IEEE, 2012, pp. 215–220.

[34] O. Ronneberger, P. Fischer, and T. Brox, "U-net: Convolutional networks for biomedical image segmentation," in *International Conference on Medical image computing and computer-assisted intervention*, Springer, 2015, pp. 234–241.

[35] X. Hu, M. A. Naiel, A. Wong, M. Lamm, and P. Fieguth, "Runet: A robust unet architecture for image super-resolution," in *Proceedings of the IEEE/CVF Conference on Computer Vision and Pattern Recognition Workshops*, 2019, pp. 0–0.

[36] K. Trebing, T. Staczyk, and S. Mehrkanoon, "Smaat-unet: Precipitation nowcasting using a small attention-unet architecture," *Pattern Recognition Letters*, vol. 145, pp. 178–186, 2021.

[37] D. Harrison, F. C. De Leo, W. J. Gallin, F. Mir, S. Marini, and S. P. Leys, "Machine learning applications of convolutional neural networks and unet architecture to predict and classify demosponge behavior," *Water*, vol. 13, no. 18, 2021, ISSN: 2073-4441. DOI: 10.3390/w13182512. [Online]. Available: https://www.mdpi.com/2073-4441/13/18/2512.

[38] S. Zagoruyko and N. Komodakis, "Wide residual networks," *arXiv preprint arXiv:1605.07146*, 2016.

[39] geeksforgeeks, *Geeksforgeeks*, 2015. [Online]. Available: https://www.geeksforgeeks.org/residual-networks-resnet-deep-learning/.

[40] J. Behrmann, W. Grathwohl, R. T. Chen, D. Duvenaud, and J.-H. Jacobsen, "Invertible residual networks," in *International Conference on Machine Learning*, PMLR, 2019, pp. 573–582.

[41] K. Zhang, M. Sun, T. X. Han, X. Yuan, L. Guo, and T. Liu, "Residual networks of residual networks: Multilevel residual networks," *IEEE Transactions on Circuits and Systems for Video Technology*, vol. 28, no. 6, pp. 1303–1314, 2017.

[42] R. Adams and L. Bischof, "Seeded region growing," *IEEE Transactions on pattern analysis and machine intelligence*, vol. 16, no. 6, pp. 641–647, 1994.

[43] P. Porwal, S. Pachade, R. Kamble, *et al.*, *Indian diabetic retinopathy image dataset (idrid)*, 2018. DOI: 10.21227/H25W98. [Online]. Available: https://dx.doi.org/10.21227/H25W98.

[44] ——, "Indian diabetic retinopathy image dataset (idrid): A database for diabetic retinopathy screening research," *Data*, vol. 3, no. 3, 2018, ISSN: 2306-5729. DOI: 10.3390/data3030025. [Online]. Available: https://www.mdpi.com/2306-5729/3/3/25.

[45] Wikipedia contributors, *Jaccard index — Wikipedia, the free encyclopedia*, [Online; accessed 27-August-2022], 2022. [Online]. Available: https://en.wikipedia.org/w/index.php?title=Jaccard_index&oldid=1105990819.

[46] MICCAI, *Miccai*, 2022. [Online]. Available: https://drac22.grand-challenge.org/.